PHYSICAL REVIEW B VOLUME 60, NUMBER 18 1 NOVEMBER 1999-II

Why $Pb(B,B')O_3$ perovskites disorder at lower temperatures than $Ba(B,B')O_3$ perovskites

B. P. Burton and E. Cockayne
Materials Science and Engineering Laboratory, Ceramics Division, National Institute of Standards and Technology, Gaithersburg, Maryland 20899

(Received 26 August 1999)

Plane-wave pseudopotential calculations of total energies were performed for three ordered perovskite related supercells in each of the eight stoichiometries of $A(B_{1/3}B'_{2/3})O_3$; $A=$Pb, Ba, $B=$Zn, Mg and, $B'=$Nb,Ta; and the eight stoichiometries of $A(B_{1/2}B'_{1/2})O_3$; $B=$Sc,In. A striking difference between the Pb and $Ba(B_{1/3}B'_{2/3})O_3$ systems is that the differences in total energies for Pb systems span ranges that are roughly an order of magnitude smaller than those for the corresponding Ba systems. This indicates much lower energetic barriers to disordering in the Pb systems, consistent with experiments. We explain this trend as a consequence of enhanced Pb-O bonding to underbonded oxygens in B^{2+}-O-B^{2+} environments. [S0163-1829(99)51642-1]

Introduction. Lead based $A(B,B')O_3$ perovskites ($A=Pb^{2+},Ba^{2+}$; $B=Mg^{2+},Zn^{2+},In^{3+},Sc^{3+}$; $B'=Nb^{5+},Ta^{5+}$) are widely used as relaxor ferroelectric[1,2] transducers, actuators, and multilayer capacitors; and their $Ba(B,B')O_3$ counterparts, particularly $Ba(Zn_{1/3}Ta_{2/3})O_3$, are the premier dielectric resonator materials.[3] Some *B*-site disorder is essential to obtain the relaxor properties of the Pb systems,[1,2] but disorder in the Ba systems can degrade the dielectric ''quality factor'' by orders of magnitude.[4,5] As indicated by the experimental data summarized in Table I, *B*-site ordering in $A(B,B')O_3$ perovskites persists to higher temperatures when the *A* cation is Ba^{2+} rather than Pb^{2+}, especially in the $A(B_{1/3}B'_{2/3})O_3$ systems.[4,6–8,10–13] Clearly, the energetics of *B*-site ordering are dramatically altered by substituting Pb for Ba on the *A* sites, and it is not obvious why this should occur. Our computational results allow us to explain this surprising result as a consequence of enhanced Pb-O hybridization between the Pb6*s* and *O* 2*p* states of underbonded oxygens in B^{2+}-O-B^{2+} or B^{2+}-O-B^{2+} environments.

All the $Ba(B_{1/3}B'_{2/3})O_3$ systems, adopt the same 1:2 crystal structure at low temperatures (a B:B':B' layer sequence perpendicular to the cubic [111] vector) but the only $Pb(B_{1/3}B'_{2/3})O_3$ system, that exhibits long-range order is $Pb(Mg_{1/3}Ta_{2/3})O_3$. When maximally ordered, the PMT 1:1 structure, has two *B* sites: one occupied by Ta; the other by a disordered $Mg_{2/3}Ta_{1/3}$ mixture. Thus, 1:1 is a partially ordered intermediate temperature phase rather than the PMT ground state (GS). In the $A(B_{1/2},B'_{1/2})O_3$ systems, all stoichiometries adopt a 1:1 structure at low temperatures, and again the $Ba(B_{1/2},B'_{1/2})O_3$ systems have higher transition temperatures for cation ordering.[10,14,19]

TABLE I. Experimental data on ordering in $A(B,B')O_3$ perovskites. $*T_t$ = cation order–disorder transition temperature.

System	Abbreviation	Observed ordering	Transition temperature range	Ref.
$Pb(Zn_{1/3},Nb_{2/3})O_3$	PZN	1:1 Short-range order		6
$Pb(Mg_{1/3},Nb_{2/3})O_3$	PMN	1:1 Short-range order		7,8
$Pb(Zn_{1/3},Ta_{2/3})O_3$	PZT	?		9
$Pb(Mg_{1/3},Ta_{2/3})O_3$	PMT	1:1⇌Disordered	$1350 < T_t^* < 1400\,^\circ$C	10
$Ba(Zn_{1/3},Nb_{2/3})O_3$	BZN	1:2⇌Disordered	$1300 < T_t < 1350\,^\circ$C	11,12
$Ba(Mg_{1/3},Nb_{2/3})O_3$	BMN	1:2⇌Disordered	$1350 < T_t < 1400\,^\circ$C	10
$Ba(Zn_{1/3},Ta_{2/3})O_3$	BZT	1:2⇌Disordered	$T_t \geqslant 1650\,^\circ$C	4
$Ba(Mg_{1/3},Ta_{2/3})O_3$	BMT	1:2⇌Disordered	$T_t \approx 1655\,^\circ$C	13
$Pb(Sc_{1/2},Nb_{1/2})O_3$	PSN	1:1⇌Disordered	$1200 < T_t < 1220\,^\circ$C	14
$Pb(Sc_{1/2},Ta_{1/2})O_3$	PST	1:1⇌Disordered	$1350 < T_t < 1400\,^\circ$C	10
$Pb(In_{1/2},Nb_{1/2})O_3$	PIN	1:1⇌Disordered	$920\,^\circ\text{C} < T_t < 950\,^\circ$C	15,16
$Pb(In_{1/2},Ta_{1/2})O_3$	PIT	1:1⇌Disordered	$1070\,^\circ\text{C} < T_t < 1100\,^\circ$C	17,18
$Ba(Sc_{1/2},Nb_{1/2})O_3$	BSN	1:1⇌Disordered	$1400\,^\circ\text{C} < T_t$	19
$Ba(Sc_{1/2},Ta_{1/2})O_3$	BST	1:1⇌Disordered	$1400\,^\circ\text{C} < T_t$	19
$Ba(In_{1/2},Nb_{1/2})O_3$	BIN	1:1	$1200\,^\circ\text{C} < T_t < 1400\,^\circ$C	20,21
$Ba(In_{1/2},Ta_{1/2})O_3$	BIT	1:1	$1200\,^\circ\text{C} < T_t < 1650\,^\circ$C	20,22

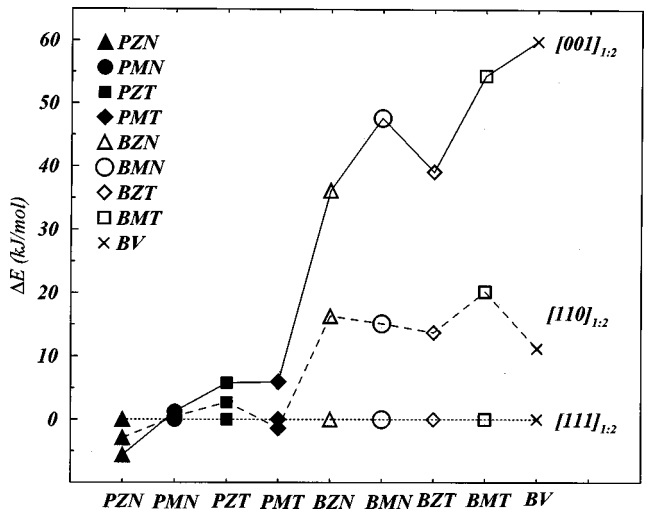

FIG. 1. Total energies (mol=ABO_3), relative to $E_{[111]_{1:2}}$, for the perovskite based supercells with compositions $A(B_{1/3}B'_{2/3})O_3$; A =Pb,Ba; B=Mg,Zn; B'=Nb,Ta; and for the ionic model of Bellaiche and Vanderbilt (BV) (Ref. 25).

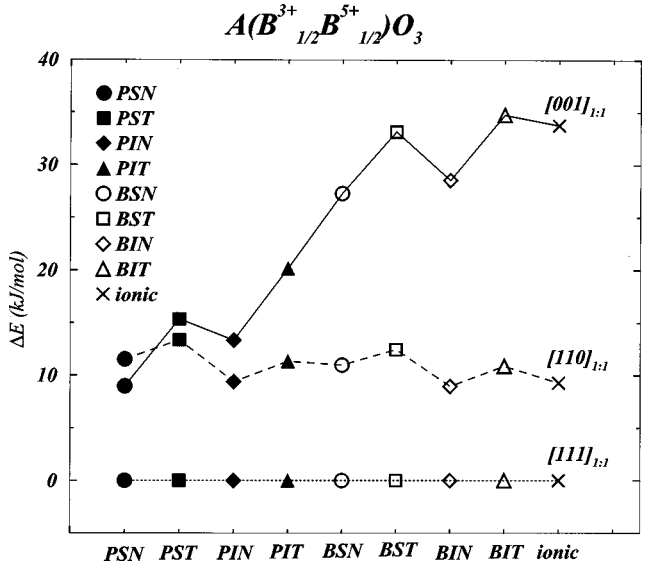

FIG. 2. Total energies, relative to $E_{[111]_{1:1}}$, for $A(B_{1/2}B'_{1/2})O_3$ perovskite based supercells.

Total-energy calculations. Total energies were calculated for three 15-atom perovskite based superstructures in each of the eight possible stoichiometries of $A(B_{1/3}B'_{2/3})O_3$; A=Pb,Ba,B=Mg,Zn,B'=Nb,Ta (Fig. 1). The three $A(B_{1/3}B'_{2/3})O_3$ superstructures ($[111]_{1:2}$,$[110]_{1:2}$, and $[001]_{1:2}$) are derived from an ideal perovskite by adding a $(B{:}B'{:}B')$ layer sequence perpendicular to the [111],[110], and [001] cubic vectors, respectively. The three 10-atom $A(B_{1/2}B'_{1/2})O_3$ superstructures, $[111]_{1:1}$,$[110]_{1:1}$, and $[001]_{1:1}$, are derived by adding $B{:}B'$ layer sequences perpendicular to the [111],[110], and [001] cubic vectors. All calculations were performed with the Vienna *ab initio* simulation program (VASP) (Ref. 23) using ultrasoft Vanderbilt[24] type plane-wave pseudopotentials with a local-density approximation for exchange and correlation energies. Electronic degrees of freedom were optimized with a conjugate gradient algorithm, and both cell constant and ionic positions were fully relaxed, but ferroelastic acentric relaxations were not investigated. Valence electron configurations for the pseudopotentials are Pb $5d^{10}6p^26s^2$ (Pb_d version); Ba $5p^66s^2$; Mg $2p^63s^2$; Zn $3d^{10}4s^2$; Sc $3p^63d4s^2$; In $4d^{10}5s^25p^1$; Nb $4p^65s4d^4$; Ta $5d^36s^2$; O$2p^6$. An energy cutoff of 395.7 eV was used, in the ''high precision'' option which guarantees that absolute energies are converged to within a few meV (a few tenths kJ/mol; mol=ABO_3). To promote cancellation of errors, formation energies for the ABO_3 and $AB'O_3$ reference states are calculated for each supercell with identical K-point meshes: $5\times5\times4$, $4\times4\times10$, and $6\times6\times2$ for $[111]_{1:2}$, $[110]_{1:2}$, and $[001]_{1:2}$ superstructures, respectively; $4\times4\times4$, $7\times7\times10$, and $8\times8\times4$ for $[111]_{1:1}$, $[110]_{1:1}$, and $[001]_{1:1}$, respectively.

VASP results for $A(B_{1/3}B'_{2/3})O_3$ supercell total energies, relative to $E_{[111]_{1:2}}$, are plotted in Fig. 1 with the corresponding supercell energies calculated with the ionic model of Bellaiche and Vanderbilt (BV),[25] in which

$$E=\frac{e^2}{2\epsilon a}\sum_{l\neq l'}\frac{\Delta q_l \Delta q_{l'}}{|l-l'|}, \tag{1}$$

where E is the total energy; e is the electron charge; ϵ is an electronic dielectric constant [$\epsilon=10$ for $A(B_{1/3}B'_{2/3})O_3$, and $\epsilon=5$ for $A(B_{1/2}B'_{1/2})O_3$]; a is the lattice constant (a =7.7 a.u., 4.07 Å);[26] Δq_l is the difference in charge between the ion at site l and the average B-site charge of +4; i.e., $\Delta q_l=-2$ for Mg^{2+} and +1 for Nb^{5+}; $a|l-l'|$ is the interionic separation. For the $A(B_{1/3}B'_{2/3})O_3$ composition, this model predicts a 1:2 GS and a $1{:}2\rightleftharpoons$ disordered transition at high temperature, consistent with the experimental data for the $Ba(B_{1/3}B'_{2/3})O_3$ systems.

In Figs. 1 and 2, the BV (ionic) model values and all the Ba systems exhibit the same hierarchies: $\Delta E_{[111]_{1:2}}<\Delta E_{[110]_{1:2}}<\Delta E_{[001]_{1:2}}$. In the Pb systems, however, this hierarchy only occurs in PMN and PZT. Experimentally, the 1:2 structure ($[111]_{1:2}$) is observed as the low temperature, presumably GS phase for all the Ba systems, and it is the predicted GS of the BV model. In the Pb systems however, the 1:2 structure may not be the GS for any of them; in PMN, for example, at least one 30-atom superstructure is predicted to have lower energy.[27] The energy ranges, $\Delta E_{[001]_{1:2}}-\Delta E_{[001]_{1:2}}$, for the BV values and the Ba systems, are between 40 and 60 kJ/mol (mol=ABO_3), but analogous ranges for the Pb systems, $\Delta E_{highest}-\Delta E_{lowest}$ are between 1 and 8 kJ/mol. In the $A(B_{1/2}B'_{1/2})O_3$ systems (Fig. 2), the ΔE ranges for the Pb systems are about half of those for the Ba systems. A second trend that occurs in both Figs. 1 and 2 is that the ΔE ranges for the $A(B,Nb)O_3$ systems are typically a little smaller than those for the corresponding $A(B,Ta)O_3$ systems, consistent with experimental data indicating higher transition temperatures for cation ordering in Ta systems (Table I).

Discussion. The configurational energy is apparently dominated by two contributions: long-range Coulomb interactions which favor configurations that maximize unlike

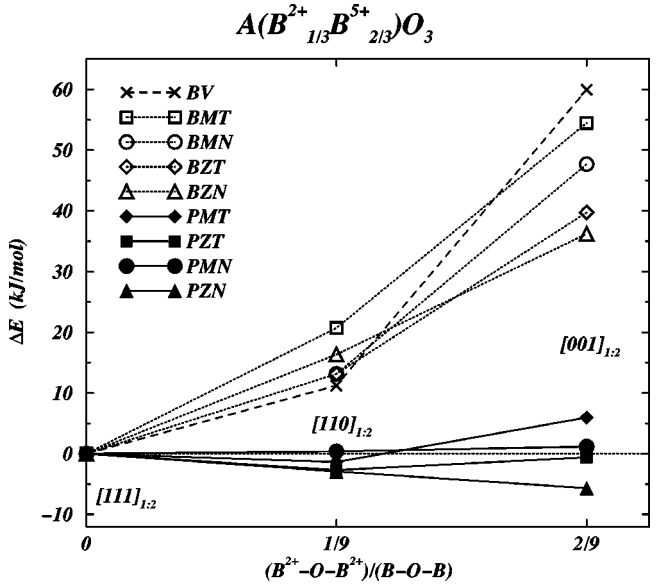

FIG. 3. ΔE vs the concentration of underbonded oxygens in the $[111]_{1:2}$, $[110]_{1:2}$, and $[001]_{1:2}$ supercells.

charges on nearest-neighbor *B*-sites, and short-range interactions that are primarily associated with the optimization of *A*-O bonds. Long-range electrostatic interactions dominate when the *A*-cation is the larger more regularly coordinated Ba^{2+}, and short-range interactions become competitive when it is the smaller less regularly coordinated Pb^{2+}.

The concentrations of underbonded oxygens in B^{2+}-O-B^{2+} or B^{3+}-O-B^{3+} environments increase monotonically in the sequences of structures $[111]_{1:2}$,$[110]_{1:2}$, and $[001]_{1:2}$ (Fig. 3), and $[111]_{1:1}$, $[110]_{1:1}$, and $[001]_{1:1}$ (Fig. 4), and in both cases, the energies for BV (ionic) model calculations and Ba systems increase monotonically as well. The Pb systems, however, do not follow this trend and the $Pb(B_{1/3},B'_{2/3})O_3$ systems depart from it more strongly than the $Pb(B_{1/2}B'_{1/2})O_3$ systems. Substitution of Pb for Ba drastically reduces the ΔE ranges, which implies that energetically favorable Pb-O interactions anticorrelate with electrostatically favorable *B*-site configurations. That is, an increase in the concentration of electrostatically destabilizing configurations implies an increase in the concentration of stabilizing Pb-O bonds, leading to a reduced change in configurational energy for the $Pb(B_{1/3},B'_{2/3})O_3$ systems. This trend is more pronounced in the $A(B_{1/3},B'_{2/3})O_3$ systems than in the $A(B_{1/2}B'_{1/2})O_3$ systems because of the larger difference in *B*-ion charges, B^{2+} and B'^{5+}vs B^{3+} and B'^{5+}, respectively. Note that in the $[110]_{1:1}$ structure (Fig. 4) the substitution of Pb for Ba causes almost no change in $\Delta E_{[110]_{1:1}}$.

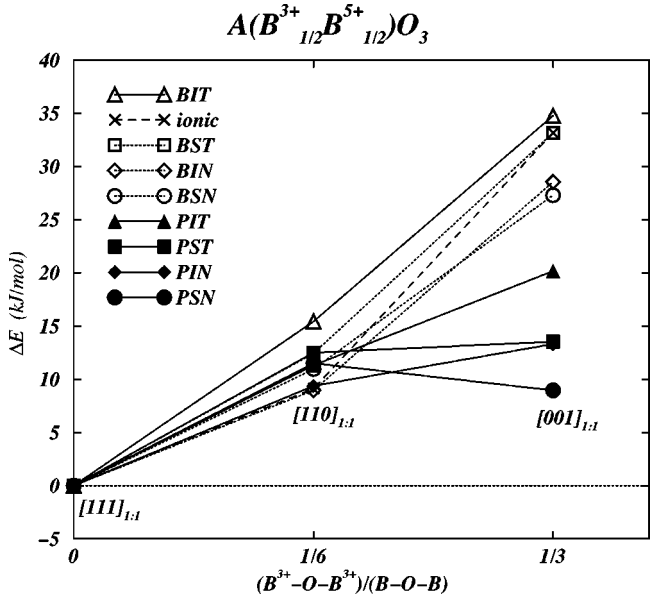

FIG. 4. ΔE vs the concentration of underbonded oxygens in the $[111]_{1:1}$, $[110]_{1:1}$, and $[001]_{1:1}$ supercells.

The most plausible explanation for these results is that hybridization of Pb 6*s* and O 2*p* states [25,28–31] stabilizes electrostatically unfavorable configurations via enhanced (short) Pb-O bonds to the otherwise underbonded oxygens in B^{2+}-O-B^{2+} or B^{3+}-O-B^{3+} triplets. Even if the GS has no underbonded oxygens, thermal disordering will create them along with overbonded oxygens in B^{5+}-O-B^{5+} triplets. In the Ba systems this energetic cost is not as strongly mitigated by short-range interactions so ordered phases are stable to higher temperatures and the supercell ΔE hierarchies for Ba systems resemble those for the BV (ionic) model. In the Pb systems however, the Pb-O bonds to underbonded oxygens typically contract, and those towards overbonded oxygens elongate (symmetry permitting).

For example, in the PMN $[110]_{1:2}$ supercell two thirds of the Pb's are in sites with only one B^{2+}-O-B^{2+} triplet (one of 12) in configuration Mg^{2+}-O-Mg^{2+}. The Pb-O bond to this oxygen is predicted to be only 2.38 Å, whereas bonds to oxygens in the other triplets are 2.62 Å for Mg^{2+}-O-Nb^{5+}, and 2.86, 3.09, and 3.36 Å for the Nb^{5+}-O-Nb^{5+} triplets. The remaining one third of Pb's in the $[110]_{1:2}$ structure have two Mg^{2+}-O-Mg^{2+} triplets (in the same $[110]_{cubic}$ plane) that compete for the short Pb-O bond and the distances to oxygens in the different triplets are all about the same: 2.83 Å for Mg^{2+}-O-Mg^{2+}; 2.85 Å for Mg^{2+}-O-Nb^{5+}; 2.79 Å for Nb^{5+}-O-Nb^{5+}. Note that $\Delta E_{[110]_{1:1}}$ (Fig. 4) is essentially unchanged by the substitution of Pb for Ba because the *B*-site coordination of Pb in this structure does not allow for the contraction of some Pb-O bonds without stretching an equal number. The importance of hybridization between O 2*p* and Pb 6*s* states in the ferroelectricity of $PbTiO_3$ was emphasized by Cohen,[28] by Cohen and Krakauer,[29] and by Bellaiche *et al.*[31] and by Wensell and Krakauer[32] in discussing the energetics of structural relaxation in PZN and BZN in the $[111]_{1:2}$ and $[001]_{1:2}$ structures.

Qualitatively, the BV model[25] captures the essence of cation ordering in the Ba systems, but it fails for the Pb systems. BV suggested that the covalency of short Pb-O bonds might provide a mechanism for stabilizing 1:1 order in place of 1:2, but no specific mechanism was described. They preferred the proposal that Pb^{4+} on *B* sites might be responsible for ''the weak 1:1 order in PMN and PMT.''[25] This is a possible contributing factor in real samples with excess lead, but it fails to explain why, in the absence of octahedral Pb^{4+}, the ΔE ranges for the $Pb(B,B')O_3$ systems are so much smaller than those of the corresponding Ba systems. Evidently, $Pb(B,B')O_3$ perovskites are more susceptible to

B-site cation disorder than their Ba counterparts because of the near cancellation of the long- and short-range contributions to the configurational energy.

Conclusions. Comparing the first-principles calculations for $Ba(B,B')O_3$ and $Pb(B,B')O_3$ perovskites indicates that the long-range Coulomb interactions which drive *B*-site ordering in Ba systems do not dominate in Pb systems. Apparently, hybridization between Pb $6s$ and O $2p$ states, on otherwise underbonded oxygens, leads to a near cancellation of long- and short-range contributions to the configurational energies of $Pb(B_{1/3},B'_{2/3})O_3$ systems, and to a partial cancellation in the $Pb(B_{1/2}B'_{1/2})O_3$ systems. This competition between long- and short-range many-body interactions explains why $Pb(B,B')O_3$ perovskites disorder at lower temperatures than $Ba(B,B')O_3$ perovskites.

Acknowledgments. The author gratefully acknowledges the assistance of G. Kresse with VASP calculations; E. Cockayne was supported by the National Research Council.

[1] N. Setter and L.E. Cross, J. Appl. Phys. **51**, 4356 (1980).
[2] L.E. Cross, Ferroelectrics **76**, 241 (1987).
[3] M.A. Akbas and P.K. Davies, in *Solid State Chemistry of Inorganic Materials*, edited by P.K. Davies, A.J. Jacobson, C.C. Torardi, and T. Vanderah, MRS Symposia Proceedings Vol. 453 (Materials Research Society, Pittsburgh, 1997).
[4] S. Kawashima, M. Nishida, I. Ueda, and H. Ouchi, J. Am. Ceram. Soc. **66**, 421 (1983).
[5] C-C. Lee, C-C. Chou, and D-S. Tsai, Ferroelectrics **206-207**, 293 (1998).
[6] C.A. Randall and A.S. Bhalla, Jpn. J. Appl. Phys., Part 1 **29**, 327 (1990).
[7] H.B. Krause, J.M. Cowley, and J. Wheatley, Acta Crystallogr., Sect. A: Cryst. Phys., Diffr., Theor. Gen. Crystallogr. **35**, 1015 (1979).
[8] J. Chen, H.M. Chan, and M. Harmer, J. Am. Ceram. Soc. **72**, 593 (1989).
[9] J. Chen, Ph.D. thesis, Lehigh University, 1991.
[10] M.A. Akbas and P.K. Davies, J. Am. Ceram. Soc. **80**, 2933 (1997).
[11] U. Treiber and S. Kemmler-Sack, J. Solid State Chem. **43**, 51 (1982).
[12] K.S. Hong, I.T. Kim, and C-D. Kim, J. Am. Ceram. Soc. **79**, 3218 (1996).
[13] R. Guo, A.S. Bhalla, and L.E. Cross, J. Appl. Phys. **75**, 4704 (1994).
[14] C.G.F. Stenger and A.J. Burggraaf, Phys. Status Solidi A **61**, 275 (1980).
[15] A. Kania, G.E. Kugel, K. Roleder, and M. Pawelczyk, Ferroelectrics **125**, 489 (1992); also, A. Kania, K. Roleder, G.E. Kugel, and M. Hafid, *ibid.* **135**, 75 (1992).
[16] N. Yasuda, H. Ohwa, J. Oohashi, K. Nomura, H. Terauchi, M. Iwata, and Y. Ishibashi, J. Phys. Soc. Jpn. **67**, 3952 (1998).
[17] A. Kania and M. Pawelczyk, Ferroelectrics **124**, 261 (1991).
[18] A.A. Bokov, I.P. Rayevsky, V.V. Neprin, and V.G. Smotrakov, Ferroelectrics **124**, 271 (1991).
[19] V.S. Filip'ev and E.G. Fesenko, Sov. Phys. Crystallogr. **10**, 532 (1966).
[20] F.S. Galasso and W. Darby, J. Chem. Phys. **66**, 131 (1962); also, F.S. Galasso, *Structure, Properties, and Preparation of Perovskite type Compounds* (Pergamon Press, Oxford, 1969).
[21] L. Brixner, J. Chem. Phys. **64**, 165 (1960).
[22] G.G. Jones, C.A. Randall, S.J. Jang, and T.R. Shrout, Ferroelectr. Lett. **12**, 55 (1990).
[23] G. Kresse and J. Hafner, Phys. Rev. B **47**, 558 (1993); G. Kresse, Ph.D. thesis, Technische Universität, Wien, 1993; G. Kresse and J. Hafner, Phys. Rev. B **49**, 14 251 (1994); G. Kresse and J. Furthmüller, Comput. Mater. Sci. **6**, 15 (1996); Phys. Rev. B **54**, 11 169 (1996); cf. http://tph.tuwien.ac.at/vasp/guide/vasp.html.
[24] D. Vanderbilt, Phys. Rev. B **41**, 7892 (1990).
[25] L. Bellaiche and D. Vanderbilt, Phys. Rev. Lett. **81**, 1318 (1998).
[26] For the $A(B_{1/3}B'_{2/3})O_3$ systems $a=7.7$ a.u. and $\epsilon=10$ as in BV. For the $A(B_{1/3}B'_{2/3})O_3$ systems $\epsilon=5$ so that $\Delta E_{[001]_{1:1}} \approx E(\mathrm{BSN})_{[001]_{1:1}} \approx E(\mathrm{BST})_{[001]_{1:1}}$.
[27] B.P. Burton (unpublished).
[28] R.E. Cohen, Nature (London) **358**, 136 (1992).
[29] R.E. Cohen and H. Krakauer, Ferroelectrics **136**, 65 (1992).
[30] L.F. Mattheiss, Phys. Rev. B **6**, 4718 (1972).
[31] L. Bellaiche, J. Padilla, and D. Vanderbilt, Phys. Rev. B **59**, 1834 (1999).
[32] M. Wensell and H. Krakauer (unpublished).